Advances in Sample Preparation 7 (2023) 100070

Contents lists available at ScienceDirect

Advances in Sample Preparation

journal homepage: www.elsevier.com/locate/sampre

Efficient analysis of polycyclic aromatic hydrocarbons by dispersive-μ-solid-phase extraction using silica-based nanostructured sorbent phases coupled to gas chromatography-mass spectrometry

Camila Scheid[a], Wendell Mello[b], Silvio Buchner[c], Edilson Valmir Benvenutti[d], Monique Deon[a,e], Josias Merib[a,e,*]

[a] Programa de Pós-Graduação em Biociências, Universidade Federal de Ciências da Saúde de Porto Alegre, Porto Alegre, RS 90050-170, Brazil
[b] Faculdade de Farmácia, Universidade Federal do Rio Grande do Sul, Porto Alegre, RS 90610-000, Brazil
[c] Instituto de Física, Universidade Federal do Rio Grande do Sul, Porto Alegre, RS, 91501-970, Brazil
[d] Instituto de Química, Universidade Federal do Rio Grande do Sul, Porto Alegre, RS, 91501-970, Brazil
[e] Departamento de Farmacociências, Universidade Federal de Ciências da Saúde de Porto Alegre, Porto Alegre, RS 90050-170, Brazil

ARTICLE INFO

Keywords:
Mesoporous silica
SBA-15
PAH
Sample preparation
Green analytical chemistry

ABSTRACT

In this study, SBA-15 mesoporous silica has been investigated as sorbent phase for the extraction and determination of 10 polycyclic aromatic hydrocarbons (PAHs) in environmental water samples for the first time. The extraction step was performed through a dispersive-μ-solid-phase extraction (D-μ-SPE) followed by gas chromatography coupled to mass spectrometry (GC-MS). In particular, the surface of SBA-15 was chemically bonded to different functional groups (aminopropyl, phenyl, octyl and octadecyl), and the extraction efficiency of each sorbent phase was investigated. The sorbent phase was synthesized and characterized by transmission electron microscopy (TEM), Fourier transform infrared spectroscopy (FTIR), N_2 sorption analysis (Brunauer–Emmett–Teller), and thermogravimetric analysis (TGA). The optimized extraction conditions consisted of using 2 mg of the sorbent SBA-15/C8, 2 mL of sample, 2 min of vortex, 4 min of stirring in orbital shaker and 1 min of centrifugation; the desorption step was performed with 25 μL of ACN:acetone (50:50 v/v), vortex for 2 min, 8 min of stirring in orbital shaker and 3 min of centrifugation. The proposed method was validated, with determination coefficients higher than 0.99 for all analytes; LODs and LOQs ranged from 0.15 to 3.03 $\mu g\ L^{-1}$ and from 0.5 to 10.0 $\mu g\ L^{-1}$, respectively; intraday precision ranged from 2.6 to 12.1%; interday precision varied from 4.5 to 25.3%; and accuracy ranged from 92.0 to 112.3 %. This methodology was successfully applied for the analysis of eight groundwater samples from monitoring wells of gas stations in São Paulo. Moreover, according to AGREEprep metrics, the proposed method can be considered sustainable according to the concepts of green analytical chemistry.

1. Introduction

Polycyclic aromatic hydrocarbons (PAHs) are a group of organic lipophilic compounds consisting of two or more aromatic rings. They are formed during the incomplete combustion of fossil fuels, tobacco, and other organic materials. PAHs can be found in soil, air, water, and food, consisting of persistent and long-lasting compounds [1]. They have gained global attention due to their persistence, high toxicity, mutagenic and carcinogenic properties, and their ability to accumulate in the environment, causing negative impacts on both the environment and human health. In particular, the aquatic environment has been greatly affected by the presence of PAHs [2].

Because PAHs are poorly soluble in water, they are present in aqueous matrices generally at trace amounts. Therefore, efficient preconcentration methods are required prior to their analysis. Classical sample preparation techniques such as solid-phase extraction (SPE) and liquid-liquid extraction (LLE) have been commonly used. However, these techniques involve multi-step and time-consuming procedures, which require large amounts of hazardous solvents. These factors raise concerns about the safety of workers and environment. More recently,

* Corresponding author at: Universidade Federal de Ciências da Saúde de Porto Alegre, 245, Sarmento Leite St., Porto Alegre RS 90050-170, Brazil.
E-mail address: josias@ufcspa.edu.br (J. Merib).

https://doi.org/10.1016/j.sampre.2023.100070
Received 25 March 2023; Received in revised form 5 May 2023; Accepted 9 May 2023

several novel techniques have been developed to address these issues by reducing solvent volumes, sorbent amount, and sample size. Notably, numerous configurations based on microextraction techniques including solid-phase microextraction and liquid-liquid microextraction have been developed for this purpose [3,4].

Dispersive micro-solid phase extraction (D-μ-SPE) is a miniaturized sample preparation technique in which a sorbent is dispersed in the sample solution through different methods such as sonication, stirring, vortexing, or shaking, permitting rapid and uniform interaction between the sorbent and analytes. The sorbent is isolated from the sample solution through filtration or centrifugation, and the analytes are eluted into a small volume of solvent before the analysis. D-μ-SPE offers advantages such as low solvent consumption, simplicity of operation, and high analyte recovery [5].

Nanostructured sorbents with high surface area can offer higher adsorption capacity than microscale materials, thereby improving the efficiency and selectivity of microextraction techniques. The development of novel sorbents is having a great impact on these techniques not only in terms of extraction efficiency and selectivity, but also enhancing the chemical or physical stability of these materials [6].

Among various nanomaterials, inorganic support comprised of mesoporous silica has been receiving a lot of attention in recent years. Santa Barbara Amorphous type 15 (SBA-15), for example, is a two-dimensional mesoporous silica discovered by Zhao and coworkers at the University of California, Santa Barbara [7]. SBA-15 is a unique silica due to its well-ordered hexagonal mesoporous structure with tunable large uniform pore sizes (up to 300 Å), high surface area (up to 1000 $m^2\ g^{-1}$), thick uniform silica walls, significant thermal stability, and ability to be functionalized [7,8]. The open pore structure of ordered mesoporous materials allows for better accessibility and more efficient diffusion of compounds compared to the pores of non-ordered materials, which may hinder molecular diffusion and access to functional groups [9].

This material has been applied in various analytical techniques including Solid-phase microextraction (SPME) and Solid-phase extraction (SPE). SBA-15 and functionalized SBA-15 have been shown to be very efficient in the extraction and preconcentration of various analytes from matrices such as water, food and biological samples [10,11]. The functionalization of mesoporous silica, in which functional groups are attached to the surface of the material, can greatly alter its physical and chemical properties. This has led to an intensive investigation of surface functionalization, as it has the potential to significantly improve the performance of mesoporous silica in a variety of applications [8,12,13]. The use of functionalized SBA-15 as sorbent in D-μ-SPE can lead to enhanced sensitivity and selectivity in the determination of PAHs. The high surface area and uniform pore size distribution of SBA-15 provide a large surface area for analyte adsorption, while the functional groups on the silica surface can effectively interact with the target analytes.

This study aimed at proposing a novel and environmentally friendly analytical methodology to determine PAHs in water samples. This approach involved the synthesis, characterization, and application of functionalized SBA-15 as extraction phase for D-μ-SPE. The separation/detection was performed by gas chromatography mass spectrometry (GC⁄-MS). In particular, sorbent phases comprised of SBA-15 functionalized with aminopropyl, phenyl, C8, and C18 were evaluated. The experimental conditions were fully optimized through multivariate and one-variable-at-a-time strategies and SBA-15/C8 was used for the validation. Additionally, the greenness of the analytical methodology was assessed through the recently proposed AGREEprep metrics.

2. Experimental

2.1. Reagents and materials

Analytical standard of PAH mix solution containing Naphthalene (Nap); 1-methylnaphthalene (1-met), 2-methylnaphthalene (2-met), Acenaphthylene (Ace), Acenaphthene (Acet), Fluorene (Flu), Phenanthrene (Phe), Anthracene (Ant), Fluoranthene (Flt) and Pyrene (Pyr) at a concentration of 2000 mg L^{-1} in acetone, and Internal standard (IS) of 2-fluorobiphenyl at a concentration of 1000 mg L^{-1} were obtained from Sigma-Aldrich (Milwaukee, USA). Stock solutions of the analytes were prepared by appropriate dilution of analytical standards in acetonitrile. IS solution was prepared by dilution in acetonitrile from Merck (Darmstadt, Germany) at 50 μg L^{-1}. All solutions were stored at -20°C. Water was purified in a Milli-Q purification system (Millipore, Bedford, USA).

The reagents used for the synthetic procedures were tetraethyl orthosilicate (TEOS), hydrochloric acid 37% (HCl), triblock copolymer (Pluronic® P123), anhydrous toluene, (3-Aminopropyl)triethoxysilane (APTES), phenyltrimethoxysilane (PhTMS), triethoxyoctylsilane (C8TES) and trimethoxy(octadecyl)silane (C18TMS) from Sigma-Aldrich (Milwaukee, USA), and anhydrous ethanol from Merck (Darmstadt, Germany).

2.2. Synthesis of the sorbent phases

The synthesis of the SBA-15 material was performed as described by Oliveira et al. [14]. Firstly, the triblock copolymer Pluronic® P123 was dissolved in a round bottom flask with HCl solution (1.6 mol L^{-1}). The mixture was then heated to 40°C with stirring and TEOS was added dropwise. The system was stirred at 40°C for 24 h. Next, it was kept in a Teflon autoclave at 100°C for another 24 h. The white solid obtained was filtered, washed with ultrapure water and dried at 80°C for 8 h. Then, the material (SBA-15) was calcined at 550°C for 6 h (heating rate of 10°C min^{-1}) to remove P123 and cleaning the pores.

SBA-15 was functionalized with four different functional groups: aminopropyl (AP), phenyl (Ph), octyl (C8), and octadecyl (C18). For grafting, 1 g of SBA-15 was dispersed in 60 mL of toluene in a round bottom flask. Then, 10 mmol of the respective organosilane was added to this mixture and stirred at 80°C for 6 h. Subsequently, the samples were centrifuged (5 min, 3500 rpm) and the supernatant was discarded. Then, the samples were first washed with 30 mL of toluene, centrifuged (5 min, 3500 rpm), and the supernatant was discarded. Next, the samples were washed twice with 30 mL ethanol, centrifuged (5 min, 3500 rpm) in each step, and filtered. They were then dried at 70°C for at least 24 h for solvent removal [15].

2.3. Characterization

The sorbent phases synthesized in this study were subjected to proper characterization to evaluate some important properties. Transmission electron microscopy (TEM) was used to assess the mesostructure and pore arrangement in a JEM-1011 microscope (JEOL) operating at an acceleration voltage of 100 kV. For sample preparation, SBA-15 powder was dispersed on isopropanol and one drop was added on a carbon-coated copper grid.

Sorption analysis was performed on Micromeritics equipment (Tristar Krypton 3020). Samples were previously degassed under vacuum at 120 °C for 12 h. Specific surface area was determined by a multipoint BET (Brunauer-Emmett-Teller) method using adsorption data. Pore volume and pore size distribution were calculated using desorption branches of nitrogen isotherms according to BJH (Barrett-Joyner-Halenda).

Structural information was obtained by Fourier transform infrared spectroscopy (FTIR) using an IR PRESTIGE21 (Shimadzu). Spectra of the silica materials were obtained in the wavenumber range of 4000-400 cm^{-1} with 32 cumulative scans and a maximum resolution of 2 cm^{-1}. Additionally, thermogravimetric Analysis (TGA) was performed using a thermoanalyser (Shimadzu Instrument model TGA-50, Kyoto, Japan), with a heating rate of 20°C min^{-1} in a 50 mL min^{-1} argon flow, from room temperature up to 900°C.

2.4. Instrumental conditions

The chromatographic analysis was performed using a GC-MS-QP 2010 Plus gas chromatograph coupled to mass spectrometry (Shimadzu, Kyoto, Japan) and autosampler model AOC-20i (Shimadzu, Kyoto, Japan). Chromatographic separation was carried out in a NST capillary column (NST, São Carlos, Brazil), model NST®-5MS (30 m × 0.25 mm × 0.25 μm film thickness). Ultrapure helium at constant flow of 1.5 mL min^{-1} was used as carrier gas. The injection temperature was set at 280°C and the initial oven temperature was set at 70°C, then it was increased to 180°C at a rate of 25°C min^{-1} and increased to 280°C (kept for 5.6 min) at a rate of 5°C min^{-1}. Automated injection was performed with a volume of 1 μL and a split ratio of 2 was employed. The mass spectrometer was operated in electron ionization (EI) mode at 70 eV. The ion source temperature and interface were set at 200°C and 280°C, respectively. The analytes were quantified using selected ion monitoring mode (SIM) with the m/z ratio of highest intensity. The retention time, some physicochemical properties of the analytes, and the m/z ratios monitored for identification and quantification are shown in Table S1 of the Supplementary Material.

2.5. Optimization of the sample preparation procedure

In order to ensure the best experimental conditions, the parameters that could affect the extraction efficiency of the target compounds were investigated using univariate and multivariate strategies. In all steps, the analytical data was submitted to statistical treatment using Statsoft Statistica 10 (Statsoft, USA) and Microsoft Excel 2016 (Microsoft, USA). This evaluation involved extractions of the compounds from blank water samples spiked with 500 µg L^{-1} of each analyte. The optimizations were employed in the following order:

(I) Initial evaluation of the sorbent type – In this step, the sorbent materials SBA-15, SBA-15/C8, SBA-15/C18, SBA-15/Ph and SBA-15/AP were evaluated in terms of extraction efficiency of PAHs through a univariate approach.
(II) Screening of the extraction variables – This optimization was assessed trough a multivariate full factorial design (2^4) using the variables mass of the sorbent phase, sample volume, extraction time and centrifugation time;
(III) Optimization of the desorption solvent - The best desorption solvent was determined using a simplex centroid design using methanol, acetonitrile and acetone;
(IV) Optimization of desorption variables – In this case, desorption time (using orbital shaker) and centrifugation time were studied through a Doehlert design.

2.6. Method validation

The method was validated according to AOAC International guidelines [16]. The analytical figures of merit were determined from external calibration curves of each compound with analyzes performed in triplicate. The coefficients of determination (r^2) were calculated based on the calibration curves tested for homoscedasticity. Limit of quantification (LOQ) was adopted as the first concentration of the linear range, and limit of detection (LOD) was obtained by dividing LOQ by 3.3. Limit of quantification (LOQ) for each analyte was experimentally determined through triplicate extractions, with coefficients of variation ≤ 20% being considered satisfactory.

Relative recovery (accuracy) and intraday and interday precisions were evaluated at 3 concentrations for each analyte. Intraday precision was determined through three extractions in the same day (n = 3), and interday precision was determined by performing three extractions per day in three different days (n = 9). The applicability of the method was evaluated by performing extractions in groundwater samples obtained from monitoring wells of gas stations in São Paulo, Brazil.

3. Results and discussion

3.1. Characterization of the sorbents

The mesostructure of SBA-15 was assessed by TEM and the obtained images are presented in Fig. 1 (A and B). The typical hexagonal arrangement of mesopores can be clearly seen, as well as the long and uniform nanochannels, confirming the successful synthesis of SBA-15. Soon after, SBA-15 was functionalized by grafting reaction with different organosilanes, aiming to incorporate functional groups with distinct chemical reactivity onto silica surface. TGA was employed to evaluate the functionalization of SBA-15, as well as to obtain information regarding the amount and thermal stability of the functional groups that were grafted onto the material. The thermograms obtained can be found in the Supplementary Material Fig. S1. The first weight loss of all sorbents, from 0 to 150°C, and it is attributed to water desorption. The second region was observed between 150 and 900 °C, where dehydroxylation reactions of silica occur by condensation of silanol groups [14], common to all sorbents. The organic decomposition occurs in this same region, where a greater mass loss was observed for all organofunctionalized silicas in comparison with SBA-15, indicating the incorporation of an organic moiety. It is notable that SBA-15/AP exhibit the highest organic content compared to the other functionalized sorbents. The SBA-15/AP sorbent had an incorporated organic content of 1.39 mmol/g, whereas the SBA-15/C8, SBA-15/C18, and SBA-15/Ph sorbents had incorporated organic contents of 0.09 mmol/g, 0.17 mmol/g, and 0.80 mmol/g, respectively. The differences in the incorporated organic content were expected and they are mainly related to the chemical nature of organosilanes, which interacts differently in the interface between silica surface (silanol groups, polar) and organic solvent (toluene, nonpolar). The hydrophobic organosilanes are more homogeneously distributed through the solvent; then, the grafting reaction occurs as a monolayer on silica surface. For APTES, due to its higher polarity, it tends to concentrate onto silica surface, which increases the incorporated organic content in the material [15]. Moreover, two other factors might be also taking place in some extent: the higher reactivity of methoxysilane groups *versus* ethoxysilane (Ph and C18 in comparison with C8 precursors); and the SBA-15 nanochannels of approximately 6 nm in diameter which can limit the diffusion of long chain molecules through the porous structure (Ph in comparison with C18 precursor).

Fig. 1 (C and D) shows the FTIR analysis of the sorbents. The spectra were splitted in two main regions for a better view. In the first region, which is depicted in Fig. 1C, a broad band arises with a maximum around 3200 cm^{-1}. This band is due to O-H stretching of the bridged silanol groups on the silica surface, as well as due to adsorbed water [16]. The SBA-15/AP, SBA-15/C8 and SBA-15/C18 sorbents exhibit the CH_2 asymmetric stretching band at 2930 cm^{-1} from the linear CH_2 chain [17]. For the SBA-15/C18, which contains the longer chain, even the symmetric CH_2 stretching band can be detected at 2860 cm^{-1} [17]. The SBA-15/Ph spectrum presents C-H stretching modes of the aromatic ring around 3070 cm^{-1} [17]. The spectra of all functionalized sorbents present the asymmetric stretching of CH_3 group at 2980 cm^{-1} [17] and the occurrence of this band was interpreted considering a fraction of unreacted methoxy groups from the organosilane reactants. In the second region, which is shown in Fig. 1D, the silica part can be clearly identified in all spectra. Strong Si-O stretching modes appear from 1200 to 1000 cm^{-1}, with a maximum at 1080 cm^{-1} [18]. The band at 960 cm^{-1} is due to the Si-OH stretching, confirming the presence of remaining silanol groups on the surface of the functionalized sorbents [18]. This band presents lower intensity for SBA-15/AP, indicating that for this sorbent the reaction occurred with a greater extension, resulting in a large degree of functionalization. These results are in accordance with TGA that shows a higher organic content. Also, the O-Si-O and Si-O-Si bending bands are clearly seen at 803 and 460 cm^{-1}, respectively [18]. In the spectrum of the SBA-15/Ph sorbent (Fig. 1D), the aromatic group can be also detected from the out-of-plane bands of the aromatic

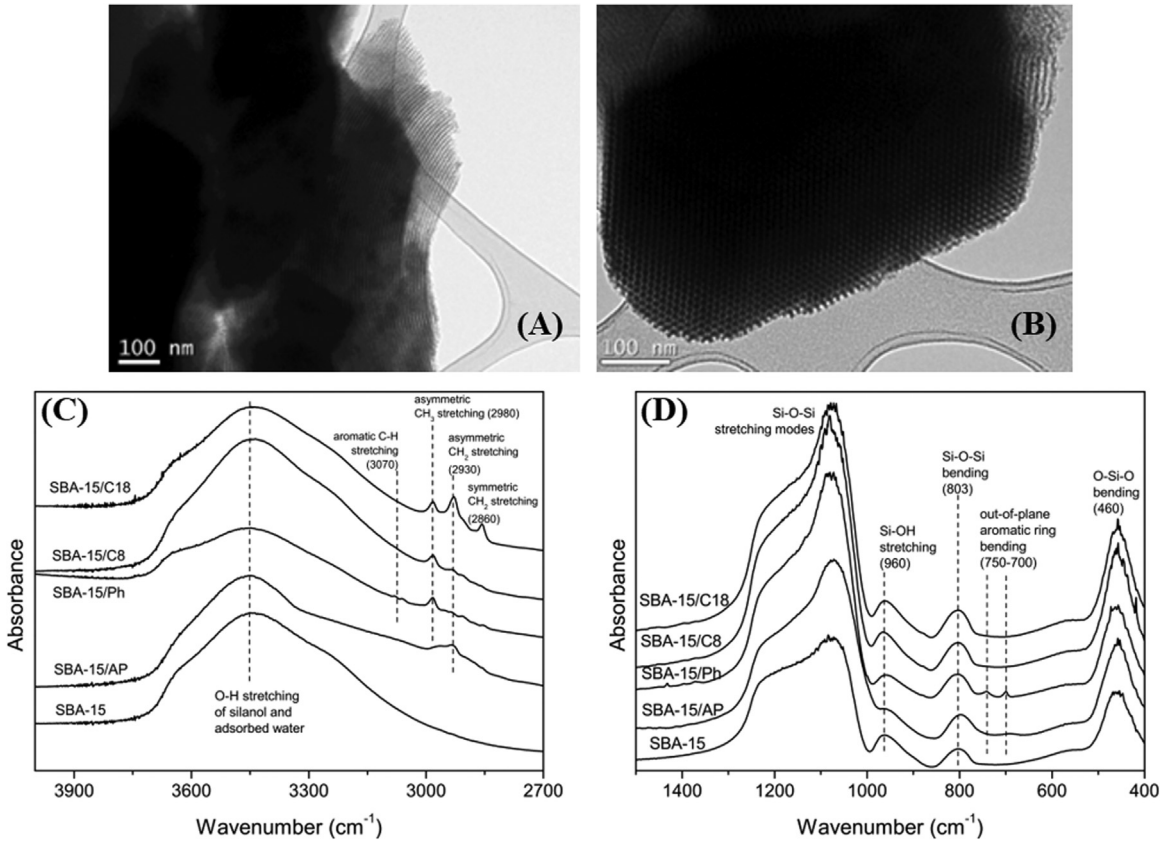

Fig. 1. Transmission Electron Microscopy of SBA-15 (A and B), and FTIR of the sorbent phases (C and D)

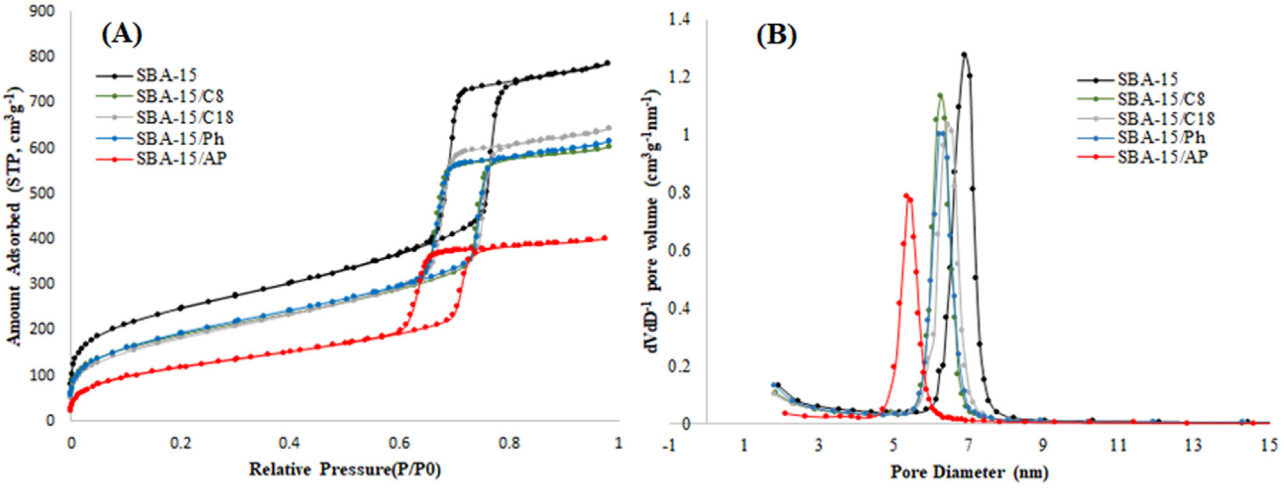

Fig. 2. Nitrogen adsorption and desorption isotherms (A) and pore size distribution of the sorbent phases (B).

ring that appear between 750 and 700 cm^{-1} [17]. Therefore, from the infrared spectra and TGA analysis it is possible to infer that the synthesis of SBA-15 and its functionalization with different functional groups were successfully attained.

In order to evaluate the porous structure of the SBA-15 before and after functionalization, N_2 adsorption-desorption isotherms and BJH pore distribution curves of the materials are shown in Fig. 2. Type IV isotherms (Fig. 2A) are observed for all materials, with parallel curves typical of H1 hysteresis [17]. In general, the H1 hysteresis loop represents a steep adsorption step indicative of capillary condensation in the pores of mesoporous silica, with the isotherm exhibiting a sharp inflection at a relative pressure P/P_0 of 0.5-0.8. This feature is characteristic of pores with cylindrical shape and uniform size [17,18]. In the analysis of BJH pore size distributions (Fig. 2B), SBA-15 exhibits a unimodal curve distribution with maximum at 6.8 nm. A decrease in pore size was observed for all sorbents compared to SBA-15, with the largest decrease for SBA-15/AP. This feature agrees with the incorporation of the organic groups by grafting reactions. Additionally, the material with the highest organic content (SBA-15/AP), is the one with the higher shift in pore size and decrease in pore volume, indicating that some pores could be also blocked due to organosilane condensation.

The BET surface areas and pore volumes are summarized in Table S2. Following the incorporation of C8, C18, Ph, and AP into SBA-15, a reduction in surface area and pore volume was noted for all materials,

which is in line with the pore walls being coated by organic monolayers, as in C8, C18 and Ph, or multilayers/blockage as in the case of AP.

The agreement between N_2 sorption analysis and TGA results emphasized that the incorporation of a greater amount of organic matter into SBA-15/AP resulted in a greater decrease in its pore size, pore volume and surface area. On the other hand, the sorbents SBA-15/C8, SBA-15/C18 and SBA-15/Ph showed only slight and similar decrease for these parameters. This data suggests that, for an extraction purpose, the materials SBA-15/C8, SBA-15/C18 and SBA-15/Ph, although presenting less chemical sites for adsorption, these sites are homogenously dispersed and more accessible along the porous structure than in SBA-15/AP. Therefore, beyond chemical affinity, diffusion of the PAHs to the adsorption site can govern the efficiency and selectivity of the sorbents prepared.

3.2. Optimization of the sample preparation procedure

3.2.1. Evaluation of the sorbent type

Sorbents used in D-μ-SPE are essential components of the extraction procedure, and their properties can have a significant impact on the efficiency and selectivity of the extraction process. Initially, in order to determine the best extraction phase for the determination of PAHs, some experiments were performed using the following strategy: 10 mg of the sorbent phase was weighted into a microtube and 3 mL of the water sample spiked with 500 μg L^{-1} of each PAH was added. 20 μL of 2-fluorobiphenyl (IS) was added at a concentration of 50 μg L^{-1} and vortexed for 2 min, followed by 20 min of stirring using an orbital shaker (300 rpm). The sample was then centrifuged (3500 rpm) for 1 min and the supernatant discarded. The desorption step was performed with 50 μL of ACN, vortexed for 2 min, then stirred for 10 min on an orbital shaker (300 rpm) and centrifuged for 1 min (3500 rpm). Finally, the organic phase was transferred to a vial and further analyzed by GC-MS.

According to the bar graph of Fig. S2, SBA-15/C8 exhibited the highest extraction efficiency for the PAHs examined; consequently, this sorbent was chosen for further studies. When evaluating the chemical structures of the compounds, it is hypothesized that two factors could influence on the extraction efficiency. Firstly, PAHs have a stronger affinity for more hydrophobic compounds, such as those present in C8, C18, and Ph functionalized materials. AP exhibits polar amino groups, resulting in lower affinity for PAHs. Additionally, SBA-15/AP has smaller surface area and pore volume, resulting in less accessible sites for PAHs adsorption. The second factor is that PAHs could be adsorbed onto the C18 and Ph material's surface, but with a stronger interaction (especially π interactions with Ph groups), which makes the desorption step less favored. In this regard, SBA-15/C8 exhibits the most favorable parameters, including homogenously distributed and accessible hydrophobic sites within the porous structure, and a suitable balance of interactions for adsorption and desorption.

3.2.2. Screening of the experimental variables

The evaluation of the parameters that can affect the extraction efficiency was performed using a 2^4 full factorial design, with four variables investigated at two levels, resulting in 16 experiments. The variables were mass of sorbent phase (2 and 10 mg), sample volume (2 and 4 mL), extraction time (4 and 20 min) and centrifugation time (1 and 5 min). The response used to generate the pareto chart was based on the geometric means of the chromatographic peak areas of the analytes in each experiment, resulting in the graph of Fig. S3. A coefficient of determination of 0.8448 was obtained, which demonstrates that the experimental results agreed with the statistical model.

According to Fig. S3, only the mass of the sorbent phase exhibited significant influence on the extraction efficiency. The negative value indicates that a lower mass of sorbent phase improves the analytical response. This result can be explained by the fact that using a lower mass, the dynamic mixture between the extraction phase and the sample is favored. On the other hand, employing higher masses, the formation of small agglomerates of the extraction phase is possible, which can affect the extraction efficiency. Therefore, 2 mg of the sorbent was selected.

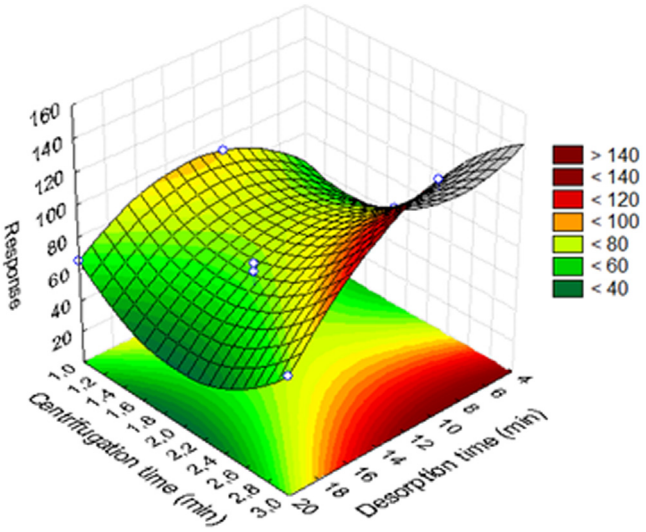

Fig. 3. Response surface for the optimization of centrifugation and desorption time of the desorption step. Sorbent phase: SBA-15/C8.

Regarding other variables (sample volume, extraction time, and centrifugation time), the results did not show statistical significance at 95% of confidence. Therefore, 2 mL of sample volume, 6 min of extraction time (vortexing for 2 min and orbital shaker for 4 min) and 1 min of centrifugation were selected as the optimal conditions for the extraction step and were fixed for the next steps of the optimization.

3.2.3. Optimization of desorption solvent type

In general, the process of liquid desorption involves the use of an organic solvent to elute or desorb the analyte from the sorbent material. The solvent must be able to break the interaction between the sorbent and analyte. Therefore, to ensure good desorption efficiency, the best solvent (or mixture of solvents) was determined, aiming at achieving the complete desorption of the PAHs from the SBA-15/C8. Table S3 of the Supplementary Material contains the different solvent ratios used in this evaluation. According to the triangular response surface obtained in Fig. S4 (r^2 = 0.8964), a mixture of ACN and acetone (50:50 v/v) exhibited the best desorption efficiency of the analytes. Therefore, this ratio was chosen as the optimal condition for further experiments.

3.2.4. Optimization of the desorption step

For this optimization, nine experiments (including a triplicate in the central point) were performed according to a Doehlert design, which centrifugation time was varied in three levels ranging from 1 to 3 min, and the desorption time (at orbital shaker) was varied in five levels from 5 to 25 min. The vortex time used in the desorption step was set at 2 min. The result of this optimization is shown in Fig. 3 (r^2 = 0.9587), and it is possible to conclude that the combination of 8 min of orbital shaker and 3 min of centrifugation provided the best results.

3.3. Optimized procedure for the determination of PAHs in water using D-μ-SPE

A general overview of the optimized analytical methodology is shown in Fig. 4. For the extraction procedure, 2 mg of SBA-15/C8 was weighted into a microtube and 2 mL of water sample was added. Then, 20 μL of 2-fluorobiphenyl (IS) was inserted at a concentration of 50 μg L^{-1} and vortexed for 2 min, followed by 4 min of stirring using an orbital shaker. The sample was then centrifuged for 1 min and the supernatant discarded. The desorption step was performed with 25 μL of ACN:acetone (50:50 v/v), vortex for 2 min, followed by 8 min of stirring

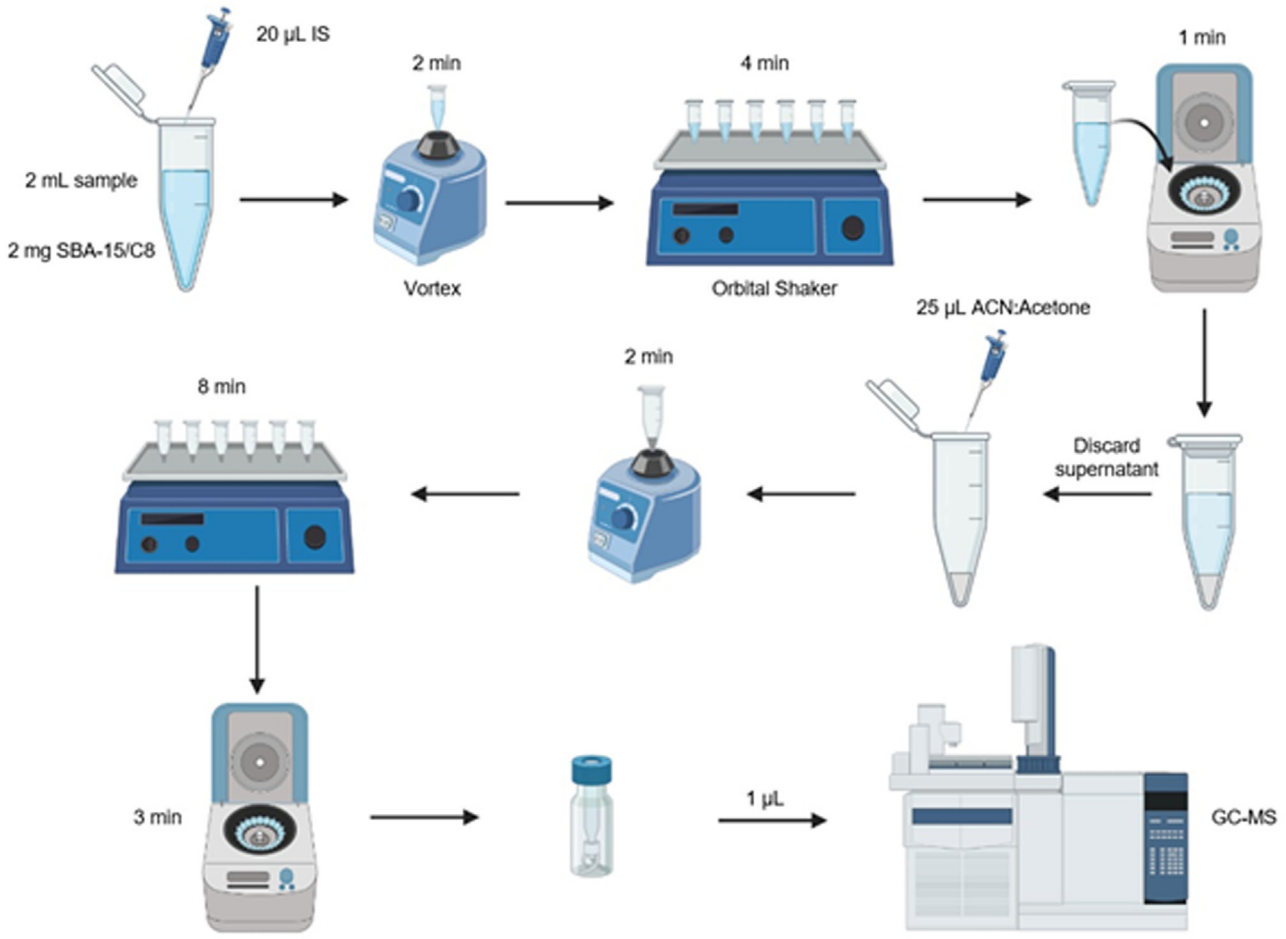

Fig. 4. Scheme of the optimized sample preparation procedure developed in this study.

Table 1
Limits of detection and quantification, linear range, weighting factor, determination coefficients and linear equation with confidence intervals (95%) for the proposed method~~,~~ using SBA-15/C8 as sorbent phase.

Analyte	LOD (µg L^{-1})	LOQ (µg L^{-1})	Linear range (µg L^{-1})	Weighting factor	r^2	Linear equation	Linear equation – confidence intervals (95%)
Nap	0.15	0.5	0.5 - 500	$1/x^2$	0.9920	y = 0.00173x + 0.00143	slope (0.001573; 0.001680) intercept (-0.009933; 0.017895)
1-met	0.15	0.5	0.5 - 500	$1/x^{1/2}$	0.9992	y = 0.00124x + 0.00038	slope (0.001111; 0.001251) intercept (-0.013857; 0.020333)
2-met	0.15	0.5	0.5 - 500	$1/y^2$	0.9971	y = 0.00139x + 0.00026	slope (0.001282; 0.001434) intercept (-0.015089; 0.022137)
Ace	0.15	0.5	0.5 - 500	$1/y^2$	0.9962	y = 0.00298x + 0.00006	slope (0.002946; 0.003189) intercept (-0.02994; 0.029138)
Acet	0.15	0.5	0.5 - 500	$1/y^2$	0.9973	y = 0.00179x – 0.00006	slope (0.001706; 0.001884) intercept (-0.018090; 0.025101)
Flu	0.30	1.0	1 - 500	$1/x^2$	0.9986	y = 0.00262x + 0.00008	slope (0.002413; 0.002734) intercept (-0.035236; 0.048152)
Phe	0.30	1.0	1 - 500	$1/x^2$	0.9966	y = 0.00559x - 0.00019	slope (0.005388; 0.005857) intercept (-0.051952; 0.07020)
Ant	0.30	1.0	1 - 500	$1/x^2$	0.9928	y = 0.00517x-0.00069	slope (0.005241; 0.005688) intercept (-0.062972; 0.053389)
Flt	3.03	10.0	10 - 500	$1/x^{1/2}$	0.9938	y = 0.01028x-0.00336	slope (0.008352; 0.012048) intercept (-0.549805; 0.589369)
Pyr	3.03	10.0	10 - 500	$1/x^2$	0.9958	y = 0.01104x + 0.00615	slope (0.009043; 0.012797) intercept (-0.548602; 0.60869)

using an orbital shaker and centrifuged for 3 min. Finally, the organic phase was transferred to a vial for further analysis by GC-MS.

3.4. Determination of the analytical parameters of merit and analysis of real samples

After the optimizations, the experimental conditions were established and the validation was performed according to the AOAC guideline [16]. The analytical figures of merit obtained employing the optimized conditions are shown in Table 1.

The determination coefficients (r^2) of the calibration curves were higher than 0.9920, which indicates good linearity. The analytes have presented heteroscedastic calibration curves, which may be explained due to the wide range of concentration. By applying weighted least squares linear regression, the resulting weighting factors are shown in Table 1. LOD values obtained for the analytes varied from 0.15 to 3.03 µg L^{-1} and LOQ varied from 0.5 to 10 µg L^{-1}.

According to Table 2, the accuracy based on the relative recoveries ranged from 92.0 to 112.3 %. Intraday precision ranged from 2.6 to 12.1 % and interday precision from 4.5 to 25.3%. Based on these results, it is possible to observe that analytes with larger chemical structures exhibited greater variability and higher limits of quantification. Particularly, analytes with larger molecular volumes may have difficult in penetrating into the pores of the sorbent phase. However, the results were very satisfactory in terms of analytical performance. Fig. S5 of the Supplementary Material shows a chromatogram obtained by GC-MS of a water sample spiked with analytes at concentration of 50 µg L^{-1}.

Table 2
Relative recovery and precisions for the target compounds in water samples analyzed by the proposed method (SBA-15/C8 as sorbent phase).

Analyte	Spiked concentration (μg L^{-1})	Relative Recovery (%) n=3	Precision (RSD, %)	
			Intraday (n=3)	Interday (n=9)
Nap	0.5	103.6	2.6	8.6
	100	95.0	9.7	10.7
	500	104.0	9.5	13.8
1-met	0.5	105.0	5.9	8.8
	100	108.9	3.6	6.5
	500	103.6	6.8	11.2
2-met	0.5	92.1	5.1	6.8
	100	106.7	4.0	5.5
	500	103.2	3.0	8.0
Ace	0.5	96.6	5.1	6.0
	100	109.5	6.7	4.5
	500	103.7	4.5	4.8
Acet	0.5	104.5	3.5	6.0
	100	112.3	4.7	6.2
	500	109.7	2.7	8.6
Flu	0.5	98.0	6.6	8.2
	100	105.7	10.0	11.2
	500	105.4	5.7	11.4
Phe	1	98.9	9.5	8.9
	100	95.5	7.7	11.9
	500	105.5	9.4	10.6
Ant	1	98.4	11.4	9.9
	100	103.4	9.2	11.4
	500	107.5	7.3	9.7
Flt	10	98.5	10.9	22.7
	100	93.4	11.7	16.3
	500	99.5	10.5	10.3
Pyr	10	94.8	9.9	25.3
	100	92.0	12.1	18.0
	500	97.0	8.0	11.0

Table 3
Comparison of the analytical features obtained with this study and other reported methods for the determination of PAHs in environmental water samples using dispersive (micro) solid-phase extraction.

Sorbent Phase	Number of PAH	Matrix	Sample volume (mL)	Amount of sorbent (mg)	Extraction time (min)	Desorption solvent/volume	Desorption time (min)	Instrumentation	LOQ (μg L^{-1})	Ref.
SBA-15/C8	10	Groundwater	2	2	6	Acetone:ACN (25 μL)	10	GC-MS	0.5-10	This study
Magnetic C18	16	Tap water	20	50	5	n-hexane (4500 μL)	-	GC-MS	-	[20]
C18	16	River and marine water	250	100	32	n-hexane (500 μL)	20	GC-MS	0.0027-0.0050	[21]
Fe_3O_4@SiO_2@Nap	7	River water	150	40	12	ACN (1000 μL)	-	HPLC-FLD	0.0015-0.004	[22]
Fe_3O_4@SiO_2@Flu	16	River, tap, and wastewater	100	40	5	n-hexane (1000 μL)	0.25	GC-FID	0.0017-0.0133	[23]
Magnetic b-CD-CNT composite	7	Rain, well, and agricultural water	10	15	20	Toluene (200 μL)	10	GC-FID	2-10	[24]
$CaCO_3$	7	Seawater	5	50	30	DCM (100 μL)	5	GC-FID	0.013-0.073	[25]
PPy.CTAB	12	River water	1.4	5	0.5	ACN:MeOH (1200 μL)	1.5	HPLC-DAD	5 - 20	[1]

After the optimization and validation, the method proposed was applied to analyze 8 groundwater samples from monitoring wells of gas stations in São Paulo. Two samples exhibited results higher than LOQ for some analytes. The first sample presented 1-met (1.21 μg L^{-1}), Phe (4.87 μg L^{-1}) and Ant (2.02 μg L^{-1}); and the second sample contained only Phe (1.11 μg L^{-1}). The analytes were not detected in other samples. Chromatograms of the analytes with concentration above LOQ can be found Fig. S6 of the Supplementary Material.

The method developed in this work was also compared to other methods reported in the literature for the determination of PAH in water using D-μ-SPE, as shown in Table 3. This method required only 2 mL of sample, whereas other methods require volumes ranging from 1.4 mL to 250 mL. Moreover, this method employs lower amounts of sorbent and organic solvent, which consequently reduces waste. Extraction and desorption times were 6 and 10 min, respectively, offering satisfactory analysis throughput. Additionally, the sorbent exhibited a straightforward and affordable synthetic procedure. Finally, limits of quantification were satisfactory for the determination of PAHs, with results lower than some of those methodologies reported in literature.

3.5. Greenness of the method

The greenness of the proposed method was evaluated using AGREEprep [19], a tool specifically designed for the assessment of analytical sample preparation greenness. This tool permits to evaluate the environmental friendliness of the methodology through a pictogram divided into ten different zones and a central zone that contains the score of the method. This score ranges from 0 to 1, with 1 being the greenest. These ten zones represent different topics of interest in green chemistry, such as energy consumption and the amount of waste generated. Each zone

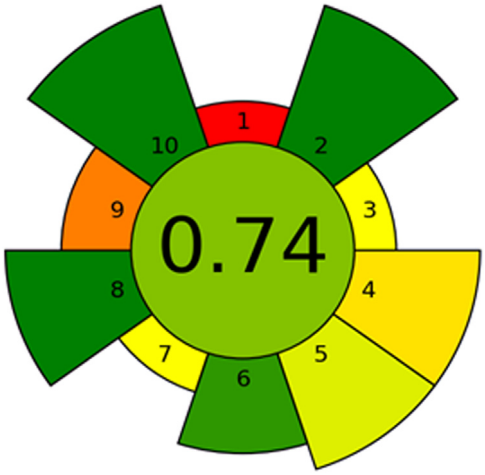

Fig 5. AGREEprep analysis of the method developed in this study.

has a different impact factor that can be changed by the user based on interest.

For the method proposed, the following topics were considered most important: use of toxic materials (zone 2) and operator safety (zone 10). Other zones considered important were: waste generation (zone 4), sample volume (zone 5), and energy consumption per sample (zone 8).

Fig. 5 shows the pictogram obtained using AGREEprep for the method proposed, as well as the score obtained (0.74). This method can be considered sustainable according to the AGREEprep tool. The main limitation is the sample preparation (zone 1), since this step is performed after the collection and transportation of the sample. In contrast, the method proposed is characterized by low reagent consumption, small number of sample preparation steps, and simplicity of the microextraction technique used. Particularly, only the sample preparation procedure was considered for this metric. It is worth mentioning that the synthetic procedure required higher volumes of solvents compared to those employed for the sample preparation workflow. Therefore, the synthesis can be considered a drawback related to the greenness of the experimental steps utilized in this investigation.

4. Conclusions

In this study, a sustainable, efficient and sensitive analytical methodology based on D-μ-SPE using nanostructured sorbent phase was proposed and fully optimized for the determination of PAHs in water samples. According to our knowledge, this is the first report of the application of nanostructured SBA-15/C8 as sorbent in D-μ-SPE for determination of PAH in water samples. The sorbent phases were successfully synthesized and comprehensively characterized, exhibiting high chemical and mechanical stabilities and SBA-15/C8 permitted to achieve satisfactory analytical parameters of merit in accordance with AOAC. It is worth mentioning that only 2 mg of sorbent phase was necessary in each extraction which emphasizes a great capability of dispersing through the aqueous sample. Additionally, this novel sorbent phase offered a rapid and environmentally friendly experimental setup in accordance with green analytical chemistry principles. Nanostructured sorbent phases consist of important trend to be comprehensively examined in dispersive-based solid phase approaches. These sorbents also exhibit structural versatility which is particularly interesting for designing novel extraction phases for specific applications.

Declaration of Competing Interest

The authors declare that they have no known competing financial interests or personal relationships that could have appeared to influence the work reported in this paper.

Data availability

Data will be made available on request.

Acknowledgements

Authors are grateful to the Brazilian governmental agency Conselho Nacional de Desenvolvimento Científico e Tecnológico (CNPq) and Universidade Federal de Ciências da Saúde de Porto Alegre (UFCSPA) for the financial support that made this research possible.

Supplementary materials

Supplementary material associated with this article can be found, in the online version, at doi:10.1016/j.sampre.2023.100070.

References

[1] F.C. Turazzi, L. Morés, E. Carasek, J. Merib, G.M. De Oliveira Barra, A rapid and environmentally friendly analytical method based on conductive polymer as extraction phase for disposable pipette extraction for the determination of hormones and polycyclic aromatic hydrocarbons in river water samples using high-performance liquid chromatography/diode array detection, J. Environ. Chem. Eng. 7 (2019), doi:10.1016/j.jece.2019.103156.

[2] J. Yu, S. Zhu, L. Pang, P. Chen, G.T. Zhu, Porphyrin-based magnetic nanocomposites for efficient extraction of polycyclic aromatic hydrocarbons from water samples, J. Chromatogr. A. 1540 (2018) 1–10, doi:10.1016/j.chroma.2018.02.006.

[3] E.F. Critto, G. Medina, M. Reta, A. Acquaviva, Determination of polycyclic aromatic hydrocarbons in surface waters by high performance liquid chromatography previous to preconcentration through solid-phase extraction by using polymeric monoliths, J. Chromatogr. A. 1679 (2022) 463397, doi:10.1016/j.chroma.2022.463397.

[4] M. Sajid, M.K. Nazal, I. Ihsanullah, Novel materials for dispersive (micro) solid-phase extraction of polycyclic aromatic hydrocarbons in environmental water samples: a review, Anal. Chim. Acta. 1141 (2021) 246–262, doi:10.1016/j.aca.2020.07.064.

[5] A. Chisvert, S. Cárdenas, R. Lucena, Dispersive micro-solid phase extraction, TrAC - Trends Anal. Chem. 112 (2019) 226–233, doi:10.1016/j.trac.2018.12.005.

[6] T. Khezeli, A. Daneshfar, Development of dispersive micro-solid phase extraction based on micro and nano sorbents, TrAC - Trends Anal. Chem. 89 (2017) 99–118, doi:10.1016/j.trac.2017.01.004.

[7] D. Zhao, J. Feng, Q. Huo, N. Melosh, G.H. Fredrickson, B.F. Chmelka, G.D. Stucky, Triblock copolymer syntheses of mesoporous silica with periodic 50 to 300 angstrom pores, Science 279 (1998) 548–552, doi:10.1126/science.279.5350.548.

[8] P. Verma, Y. Kuwahara, K. Mori, R. Raja, H. Yamashita, Functionalized mesoporous SBA-15 silica: recent trends and catalytic applications, Nanoscale 12 (2020) 11333–11363, doi:10.1039/d0nr00732c.

[9] K. Lan, D. Zhao, Functional ordered mesoporous materials: present and future, Nano Lett. 22 (2022) 3177–3179, doi:10.1021/acs.nanolett.2c00902.

[10] M.M. Abolghasemi, S. Hassani, M. Bamorowat, Efficient solid-phase microextraction of triazole pesticides from natural water samples using a Nafion-loaded trimethylsilane-modified mesoporous silica coating of type SBA-15, Microchim. Acta. 183 (2016) 889–895, doi:10.1007/s00604-015-1724-0.

[11] D. Wang, X. Chen, J. Feng, M. Sun, Recent advances of ordered mesoporous silica materials for solid-phase extraction, J. Chromatogr. A. 1675 (2022) 463157, doi:10.1016/j.chroma.2022.463157.

[12] E.F. Aboelfetoh, M.E. Z. Elabedien, E.Z.M. Ebeid, Effective treatment of industrial wastewater applying SBA-15 mesoporous silica modified with graphene oxide and hematite nanoparticles, J. Environ. Chem. Eng. 9 (2021) 104817, doi:10.1016/j.jece.2020.104817.

[13] S. Nasreen, U. Rafique, S Ehrman, M.A. Ashraf, Synthesis and characterization of mesoporous silica nanoparticles for environmental remediation of metals, PAHs and phenols, Ekoloji 27 (2018) 1625–1637.

[14] M.R. Oliveira, M. Deon, E.V. Benvenutti, V.A. Barros, D.C. de Melo, E. Franceschi, S.M. Egues, J.F. De Conto, Effect of microwave irradiation on the structural, chemical, and hydrophilicity characteristics of ordered mesoporous silica SBA-15, J. Sol-Gel Sci. Technol. 94 (2020) 708–718, doi:10.1007/s10971-020-05219-w.

[15] J. O.N. Ribeiro, E.H.M. Nunes, D.C.L. Vasconcelos, W.L. Vasconcelos, J.F. Nascimento, W.M. Grava, P.W.J. Derks, Role of the type of grafting solvent and its removal process on APTES functionalization onto SBA-15 silica for CO2 adsorption, J. Porous Mater. 26 (2019) 1581–1591, doi:10.1007/s10934-019-00754-6.

[16] AOAC Official Methods of Analysis Appendix F: Guidelines for Standard Method Performance Requirements. http://www.eoma.aoac.org/app_f.pdf., 2016 (accessed 10 February 2023).

[17] M. Thommes, K. Kaneko, A.V. Neimark, J.P. Olivier, F. Rodriguez-Reinoso, J. Rouquerol, K.S.W. Sing, Physisorption of gases, with special reference to the evaluation of surface area and pore size distribution (IUPAC Technical Report), Pure Appl. Chem. 87 (2015) 1051–1069, doi:10.1515/pac-2014-1117.

[18] K.S.W. Sing, D.H. Everett, R.A.W. Haul, L. Moscou, R.A. Pierotti, J. Rouquerol, T. Siemieniewska, Reporting physisorption data for gas/solid systems with special reference to the determination of surface area and porosity (recommendations 1984), Pure Appl. Chem. 57 (1985) 603–619.

[19] F. Pena-Pereira, M. Tobiszewski, W. Wojnowski, E. Psillakis, A tutorial on AGREEprep an analytical greenness metric for sample preparation, Adv. Sample Prep. 3 (2022) 100025, doi:10.1016/j.sampre.2022.100025.
[20] Y. Liu, H. Li, J.M. Lin, Magnetic solid-phase extraction based on octadecyl functionalization of monodisperse magnetic ferrite microspheres for the determination of polycyclic aromatic hydrocarbons in aqueous samples coupled with gas chromatography-mass spectrometry, Talanta 77 (2009) 1037–1042, doi:10.1016/j.talanta.2008.08.013.
[21] M.M. Nascimento, G.O. Rocha, J.B. Andrade, Simple and effective dispersive micro-solid phase extraction procedure for simultaneous determination of polycyclic aromatic compounds in fresh and marine waters, Talanta 204 (2019) 776–791, doi:10.1016/j.talanta.2019.06.061.
[22] Y. Cai, Z.H. Yan, N.Y. Wang, Q.Y. Cai, S.Z. Yao, Preparation of naphthyl functionalized magnetic nanoparticles for extraction of polycyclic aromatic hydrocarbons from river waters, RSC Adv. 5 (2015) 56189–56197, doi:10.1039/c5ra10054b.
[23] Y. Cai, Z. Yan, M. NguyenVan, L. Wang, Q. Cai, Magnetic solid phase extraction and gas chromatography-mass spectrometrical analysis of sixteen polycyclic aromatic hydrocarbons, J. Chromatogr. A. 1406 (2015) 40–47, doi:10.1016/j.chroma.2015.06.024.
[24] M. Yazdanpanah, S. Nojavan, Micro-solid phase extraction of some polycyclic aromatic hydrocarbons from environmental water samples using magnetic β-cyclodextrin-carbon nano-tube composite as a sorbent, J. Chromatogr. A. 1585 (2019) 34–45, doi:10.1016/j.chroma.2018.11.066.
[25] A.A. Nuhu, C. Basheer, A.A. Shaikh, A.R. Al-Arfaj, Determination of polycyclic aromatic hydrocarbons in water using nanoporous material prepared from waste avian egg shell, J. Nanomater. (2012) 2012, doi:10.1155/2012/305691.